

# Achieving High-Resolution Hard X-ray Microscopy using Monolithic 2D Multilayer Laue Lenses

W. Xu, E. Nazaretski

To be published in "Microscopy Today"

November 2022

Photon Sciences

**Brookhaven National Laboratory**

**U.S. Department of Energy**

USDOE Office of Science (SC), Basic Energy Sciences (BES) (SC-22)

Notice: This manuscript has been authored by employees of Brookhaven Science Associates, LLC under Contract No. DE-SC0012704 with the U.S. Department of Energy. The publisher by accepting the manuscript for publication acknowledges that the United States Government retains a non-exclusive, paid-up, irrevocable, world-wide license to publish or reproduce the published form of this manuscript, or allow others to do so, for United States Government purposes.

## **DISCLAIMER**

This report was prepared as an account of work sponsored by an agency of the United States Government. Neither the United States Government nor any agency thereof, nor any of their employees, nor any of their contractors, subcontractors, or their employees, makes any warranty, express or implied, or assumes any legal liability or responsibility for the accuracy, completeness, or any third party's use or the results of such use of any information, apparatus, product, or process disclosed, or represents that its use would not infringe privately owned rights. Reference herein to any specific commercial product, process, or service by trade name, trademark, manufacturer, or otherwise, does not necessarily constitute or imply its endorsement, recommendation, or favoring by the United States Government or any agency thereof or its contractors or subcontractors. The views and opinions of authors expressed herein do not necessarily state or reflect those of the United States Government or any agency thereof.

# Achieving High-Resolution Hard X-ray Microscopy using Monolithic 2D Multilayer Laue Lenses

Wei Xu<sup>1</sup>, Weihe Xu<sup>1</sup>, Nathalie Bouet<sup>1</sup>, Juan Zhou<sup>1</sup>, Hanfei Yan<sup>1</sup>, Xiaojing Huang<sup>1</sup>, Ming Lu<sup>2</sup>, Maxim Zalalutdinov<sup>3</sup>, Yong S. Chu<sup>1</sup>, and Evgeny Nazaretski<sup>1,\*</sup>

<sup>1</sup> National Synchrotron Light Source II, Brookhaven National Laboratory, Upton, NY 11973, USA

<sup>2</sup> Center for Functional Nanomaterials, Brookhaven National Laboratory, Upton, NY 11973, USA

<sup>3</sup> Naval Research Laboratory, Washington, DC 20375, USA

\* [enazaretski@bnl.gov](mailto:enazaretski@bnl.gov)

**Abstract:** This article introduces the 2D multilayer Laue lens (MLL) nanofocusing optics we recently developed for high-resolution hard x-ray microscopy. The new optics utilized a Micro-Electro-Mechanical-Systems (MEMS) - based template to accommodate two linear MLL optics in a pre-aligned configuration. The angular misalignment between two lenses was controlled in tens of millidegrees, and the lateral position error was on a micrometer scale. Using the developed 2D MLLs, we have demonstrated an astigmatism-free point focus of approximately 14 nm by 13 nm in horizontal and vertical directions, respectively, at 13.6 keV photon energy. The success of 2D MLL optics with an approaching 10 nm resolution is a significant step forward for the development of high-resolution hard x-ray microscopy and applications of MLL optics in the hard x-ray community.

**Keywords:** X-ray microscopy, multilayer Laue lenses, optics, MEMS, microfabrication

## Introduction

X-ray microscopy is a powerful characterization tool applied in many scientific fields, such as materials science, environmental science, biology, and energy research [1–4]. With the advances in synchrotron source brilliance and efficient x-ray focusing optics, significant progress has been made to apply x-ray beams for nanoscale analysis. X-rays with high photon energies (typically above several keVs) are called hard x-rays, which have sufficient penetration depth and depth of focus for most of the nanoscale specimen, while providing an excellent imaging resolution. However, imaging with hard x-rays faces challenges in both optics and microscopy systems. The mostly-used optics for x-ray nanofocusing include Fresnel zone plates, Kirkpatrick-Baez (KB) mirrors, and multilayer Laue lenses (MLLs) [5–7]. Among others, MLLs have been proposed and employed for high-efficiency nanofocusing in the hard x-ray regime [8–10]. MLLs are diffractive optics made of layers of alternating materials with different refractive indices (e.g., WSi<sub>2</sub>/Si, W/SiC, and WC/SiC). Since MLLs are one-dimensional focusing elements, in order to achieve point focusing, two MLLs must be orthogonally aligned with one another [11] (Figure 1). This involves eight independent motions with nanoscale resolutions. For instance, to maintain a 10 nm diffraction-limited point focus, the tolerance for orthogonal misalignment should be less than 0.01°, and the distance between the focal planes of two MLLs should be less than the depth of focus (e.g., ~2 μm) [12]. Moreover, when nm-scale spatial resolution imaging is considered, the stability of the MLLs and their alignment also needs to be maintained for the experiments. Those requirements pose significant technical challenges for a microscopy system itself and require an extremely complex and stable instrument.

Several sophisticated MLL-based instruments have been designed, constructed, and commissioned in recent years[13–17]. For instance, a high-resolution scanning hard x-ray microscope has been developed at the Hard X-ray Nanoprobe (HXN) beamline of the National Synchrotron Light Source II (NSLS-II) (Figure 2). It utilizes two individual MLL nanofocusing optics to provide non-destructive chemical mapping with unprecedented spatial resolution approaching 10 nm in 2D and 3D [5,17,18]. The HXN endstation utilizes state-of-the-art piezo-mechanical components and offers positioning accuracy of just a few nanometers. While it works well for many experiments, the alignment procedure of two individual MLLs in the current system is rather complex. Moreover, when performing focusing experiments below 10 nm, space constraints start to play a role making alignment even more complex.

The development of a monolithic pre-aligned 2D MLL nanofocusing optic could minimize degrees of the nanoscale motion needed for MLL alignment and substantially reduce the complexity of an instrument. Over the past few years, many initiatives have been made to develop monolithic 2D MLL optics [19–22], such as UV-adhesive assisted direct bonding of MLL structures. However, uncontrollable stress and potential contamination from UV adhesives make the direct bonding approach very difficult.

In this article, we report our recently developed monolithic MEMS-based 2D MLL nanofocusing optics for high-resolution hard x-ray microscopy [23]. By utilizing microfabrication technologies, we have manufactured MEMS-based silicon templates to accommodate two linear MLL optics in a pre-aligned configuration, which significantly simplify the MLLs alignment process. Using the developed 2D MLL structure, we have demonstrated an astigmatism-free point focus of ~14 nm by ~13 nm in horizontal and vertical directions, respectively, at 13.6 keV photon energy. The new system dramatically alleviates the design constraints and complexity of the MLL microscope. Furthermore, due to the reduced complexity, the new system is compatible with more conventional and widely used zoneplate-based x-ray microscopy systems, making high-resolution x-ray imaging more accessible at other synchrotron facilities.

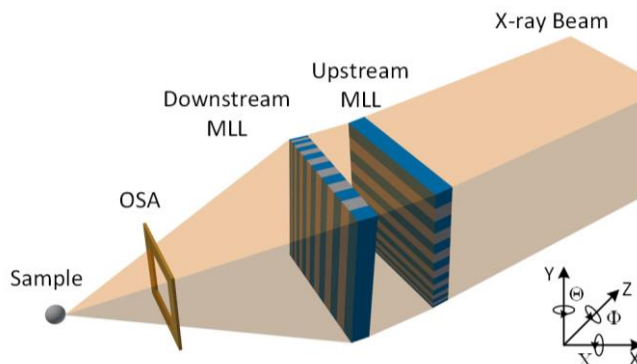


**Figure 1:** Schematic of MLL-based x-ray microscope. A total of eight degrees of rotational and translational motions are required to perform full alignment of two linear MLLs. A central beamstop is not shown in the schematic.

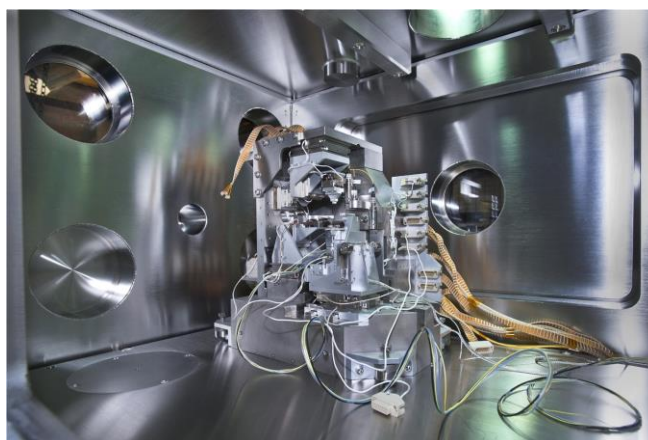


**Figure 2:** The MLL microscope module at Hard X-ray Nanoprobe (HXN) beamline of the National Synchrotron Light Source II (NSLS-II).

## Methods and Materials

**Design of MEMS-based 2D MLL optics.** We designed a MEMS-based 2D MLL x-ray nanofocusing optics by utilizing microfabrication techniques [23,24]. As shown in Figure 3, the entire optics consists of a MEMS template, two linear MLLs, and two adapters. The MEMS template, which is fabricated on a  $\sim 500\ \mu\text{m}$  thick silicon wafer, has linear dimensions of  $\sim 10 \times 10 \times 0.5\ \text{mm}^3$ . On each side of the template, there is a microfabricated holding slot, which includes multiple alignment ‘teeth’ and cantilever-typed silicon springs. Two holding slots on the front and back sides of the wafer are aligned orthogonally with a well-defined angle. There is an etched-through aperture at the center of the template. MLLs are accommodated in the holding slot, one on each side. Adapters are used if the sizes of MLLs do not fit into the holding slot. The mounted MLLs align to the alignment ‘teeth’ and are pushed by the springs to secure their positions. The active optical regions of two MLL optics overlap at the aperture, where the x-ray beam passes through to illuminate both MLLs.

The position of the MLLs mounted onto the template is precisely controlled by leveraging the high accuracy provided by microfabrication techniques. The angular position of the mounted MLLs is adjusted through the alignment teeth. By changing the length and distance of adjacent alignment teeth, we can change the angle between two slots and, consequently, the orthogonality of MLLs mounted in the slots. The separation distance between two lenses is adjusted by changing the depth of etched holding slots or the thickness of adapters so that it agrees with the focal length differences of two individual MLLs in order to achieve astigmatism-free point focus. For design details, please see our previous publications [23,24].

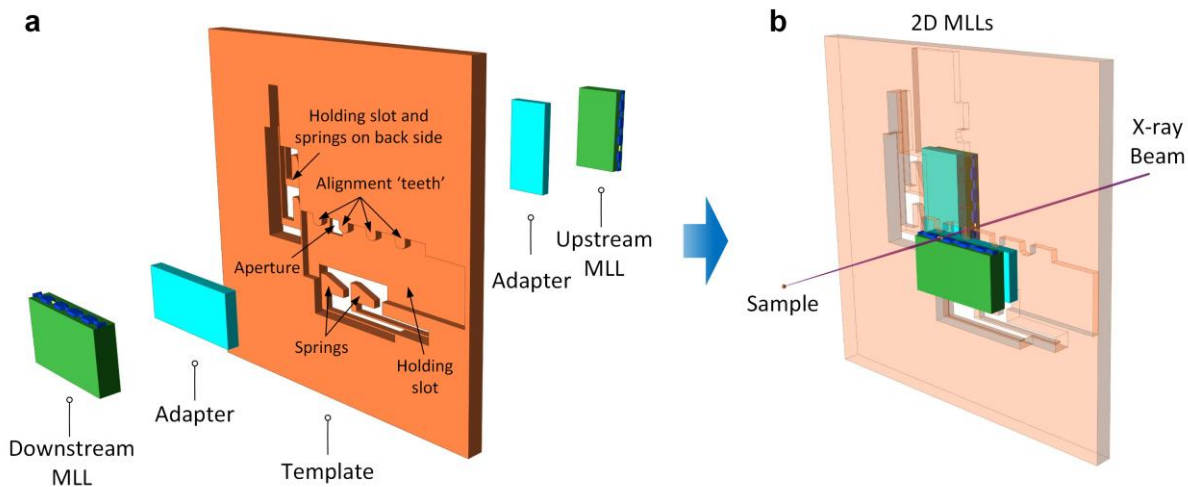


**Figure 3:** MEMS-based 2D MLL x-ray nanofocusing optics. (a) A MEMS template shows the key features, including holding slots, alignment ‘teeth’, springs, and an aperture. (b) 2D MLL optics assembled using the MEMS template. X-ray beam passes through the aperture, illuminates two overlapping MLLs, and focuses on the sample. Adapted with permission [23]. Copyright 2020, Optica Publishing Group.

**Fabrication of MEMS-based templates.** The MEMS templates were fabricated through a microfabrication process, which includes multiple steps of photolithography and deep reactive-ion etching (DRIE). The fabrication details are included in our previous publications [23,24].

**Fabrication of MLL optics.** The MLL optics were fabricated via magnetron sputtering deposition on a silicon substrate and further sectioned by reactive ion etching followed by the

focused ion beam (FIB) milling. The fabricated MLL optics were then characterized with respect to dimensions, morphology, and optical properties by using optical microscopy, SEM, and interferometer.

**Assembly of 2D MLL optics.** Upon completion of the fabrication of MLL optics and MEMS templates, we mounted the 1D lenses onto the template and characterized the developed 2D MLL optics with respect to orthogonality, separation distance, and stability. The orthogonality of the assembled 2D MLL was adjusted by changing templates. The separation distance of the assembled MLLs was characterized by using a white-light interferometer. The lateral position of two MLLs was adjusted under an optical microscope to have their zone areas overlap through the template aperture.

## Results

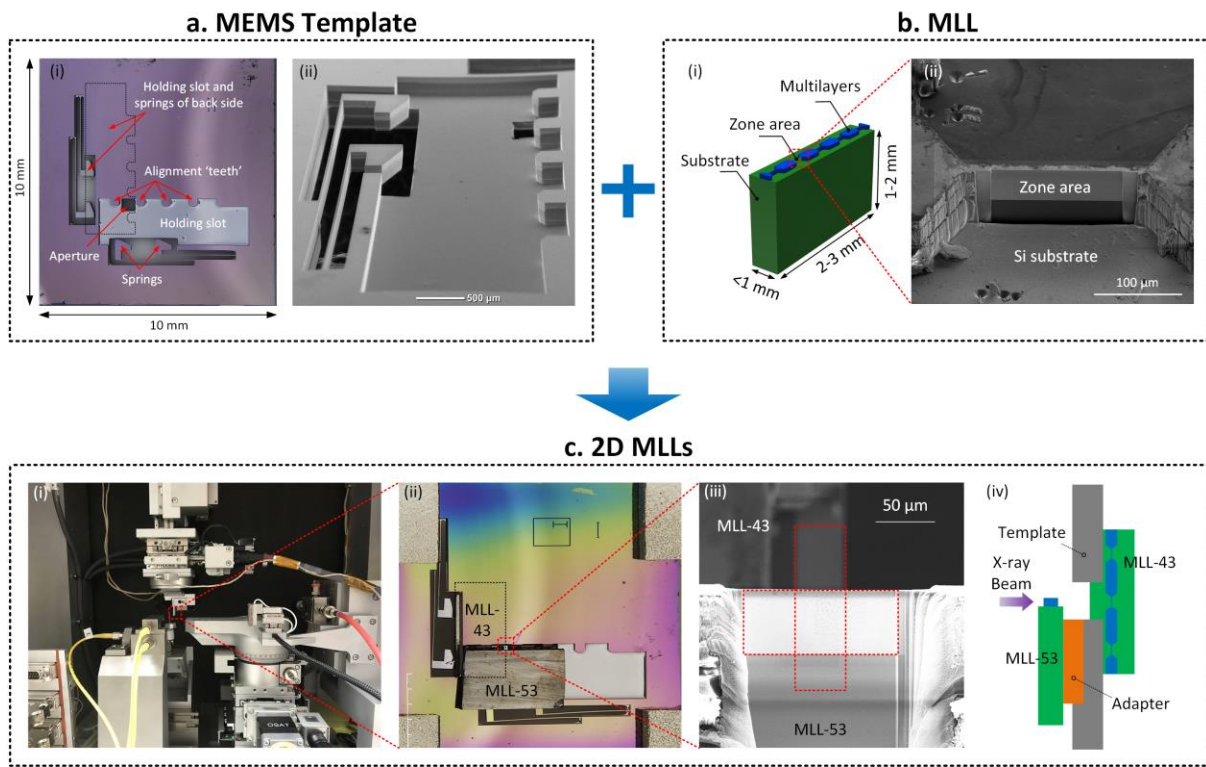


**Figure 4:** (a) Microfabricated MEMS template ((i) The optical image, (ii) SEM image of the holding slot). (b) MLL optics ((i) Schematic of an MLL. (ii) SEM image of the focused-ion-beam (FIB)-etched zone area of the lens). (c) Assembled 2D MLL optics ((i) the apparatus with mounted 2D MLL optics for x-ray focusing, (ii) 2D MLLs, (iii) Overlapped zone areas, (iv) 2D MLLs configuration. Adapted with permission [23]. Copyright 2020, Optica Publishing Group.

**MEMS template.** Figure 4a shows an example of the microfabricated silicon template [23,24]. The overall lateral dimensions are  $\sim 10 \times 10 \text{ mm}^2$ . On each side of the template, there is an etched holding slot, along with alignment teeth and springs. Two holding slots on the front and back sides are aligned orthogonally to each other. Figure 4a-ii shows an SEM image of the holding slot. The etching depth of slots depends on the used MLLs, typically between 150 and 250  $\mu\text{m}$ . It can be modified by changing the number of etching cycles with a submicron resolution. By changing the length difference of adjacent alignment teeth, we have fabricated a set of templates with the angle

between two slots gradually changed from  $89.7^\circ$  to  $90.3^\circ$  with an angular increment of  $\sim 25$  millidegrees. By using a template with the most appropriate slot angle, we can minimize the angular misalignment induced by the various factors. The template can directly accommodate most of the MLLs we have, which have a height of  $\sim 1.5$  mm. For MLLs that could not be directly mounted into the slot, we will use an adapter, which will be bonded with the MLL first, and then the entire piece will be mounted into the slot.

**MLL optics.** Figure 4b-i shows the schematic of the fabricated MLL optics. The MLL optics typically have dimensions of 2-3 mm long, 1-2 mm high, and less than 1 mm thick. It includes a silicon substrate and deposited Si/WSi<sub>2</sub> multilayers, in which there is a FIB polished zone area used for x-ray focusing. Figure 4b-ii shows an example of the FIB polished zone area of MLL optics. The two MLLs used in this work have aperture sizes (thickness of multilayer structure) of  $53\ \mu\text{m}$  (MLL-53) and  $43\ \mu\text{m}$  (MLL-43), respectively [23]. The thinnest zone is 4 nm for both lenses. The focal length for the upstream (MLL-53) and downstream (MLL-43) lenses is estimated to be around  $5200\ \mu\text{m}$  and  $4200\ \mu\text{m}$ , respectively, for 12 keV photon energy.

**2D MLLs.** Upon completion of the fabrication of MLL optics and MEMS templates, we assembled the 1D lenses onto the template. Figure 4c shows an example of 2D MLLs, which were mounted on a dedicated apparatus for x-ray focusing characterization [23]. There were two MLLs assembled on the template, one on each side. The positions of the zone area of the two lenses were adjusted to overlap each other under an optical microscope. The angular misalignment between two MLLs was determined to be  $\sim 6$  millidegrees, and the separation distance between two MLLs was  $\sim 1050\ \mu\text{m}$ .

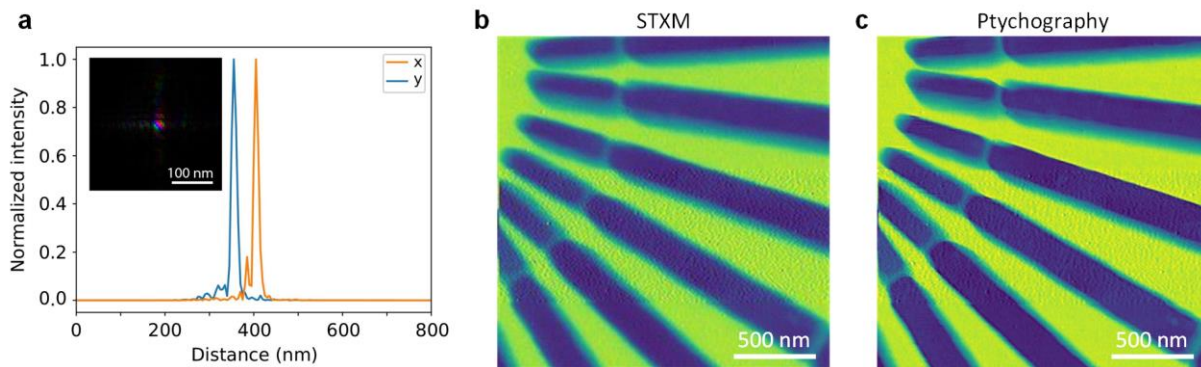


**Figure 5:** X-ray focusing performance of monolithic MEMS-based MLL optics. **a** Results of ptychography measurements. A point focus of  $\sim 14$  nm and  $\sim 13$  nm in horizontal and vertical directions has been reconstructed. The inset shows the shape of a probe with the amplitude being displayed with brightness and the phase with color. **b** Scanning Transmission x-ray Microscopy (STXM) image formed by plotting the total transmission as a function of sample position. **c** ptychography (amplitude) image for the STXM measurement. The smallest features of 20 nm (gaps between inner and outer spokes) can be resolved. Adapted with permission [23]. Copyright 2020, Optica Publishing Group.

**X-ray focusing performance.** The focusing performance of the developed 2D MLL optics was evaluated at the Hard X-ray Nanoprobe (HXN) Beamline at the National Synchrotron Light Source II (NSLS-II) [17]. The monolithic structure was mounted in a dedicated apparatus used for optics characterization [15]. Ptychography has been used for point-focus evaluation. The reconstructed line-focusing profiles for horizontal and vertical directions yielded the full width half maximum values of  $\sim 14$  nm and  $\sim 13$  nm, respectively, as shown in Figure 5a [23]. The inset

in Figure 5a represents the reconstructed x-ray wavefront at its focal plane, with the phase shown in color and the amplitude in brightness. Since the majority of intensity is confined within the central peak with just modest side-lobes, the optics are ideal for direct (transmission or fluorescence) high-resolution imaging. Figure 5b demonstrates the absorption contrast (STXM) image produced by plotting the total transmission as a function of the sample (Siemens star) position. Figure 5c illustrates the amplitude of the simultaneous ptychography image for comparison. The 20 nm gaps between inner and outer spokes, which are the tiniest features, can be clearly resolved.

## Conclusion

The developed monolithic MEMS-based 2D multilayer Laue lens nanofocusing optics significantly simplify the MLLs alignment process and meanwhile guarantee the angular and lateral alignment of assembled 2D optics. At 13.6 keV photon energy, the x-ray ptychography measurements yielded astigmatism-free point focusing of ~14 nm and ~13 nm in horizontal and vertical directions, respectively. The new 2D optics remarkably reduces the complexity of current MLL microscopes and makes 2D MLLs compatible with conventional zone plate-based scanning x-ray microscopes. Any synchrotron facility that operates a zone plate-based microscope and is interested in high-resolution hard x-ray imaging could benefit from this new focusing device to improve imaging capabilities. The developed 2D MEMS-based MLL optic is a significant step forward in bringing robust, compact, user-friendly, high-resolution hard x-ray imaging capabilities to synchrotron- and potentially lab-based x-ray microscopes.

## Acknowledgments

This work was partially carried out at the Center for Functional Nanomaterials, Brookhaven National Laboratory, which was supported by the U.S. Department of Energy, Office of Basic Energy Sciences, under Contract No. DE-SC0012704 and used resources of the National Synchrotron Light Source II, a U.S. Department of Energy (DOE) Office of Science User Facility operated for the DOE Office of Science by Brookhaven National Laboratory under Contract No. DE-SC0012704. This work was also performed in part at the Advanced Science Research Center NanoFabrication Facility of the Graduate Center at the City University of New York.

## References

- [1] DA Shapiro et al., *Nat Photonics* 8 (2014) <https://doi.org/10.1038/nphoton.2014.207>.
- [2] X Liu et al., *ACS Appl Nano Mater* 2 (2019) <https://doi.org/10.1021/acsanm.8b02309>.
- [3] FT Ling et al., *Sci Rep* 8 (2018) <https://doi.org/10.1038/s41598-018-31335-3>.
- [4] I Calvo-Almazán et al., *IEEE J Photovolt* 9 (2019) <https://doi.org/10.1109/JPHOTOV.2019.2942487>.
- [5] H Yan et al., *Nano Futur* 2 (2018) <https://doi.org/10.1088/2399-1984/aab25d>.
- [6] M Holler et al., *Rev Sci Instrum* 89 (2018) <https://doi.org/10.1063/1.5020247>.
- [7] E Nazaretski et al., *J Synchrotron Radiat* 29 (2022) <https://doi.org/10.1107/S1600577522007056>.
- [8] HC Kang et al., *Appl Phys Lett* 92 (2008) <https://doi.org/10.1063/1.2912503>.
- [9] R Conley et al., *Synchrotron Radiat News* 29 (2016) <https://doi.org/10.1080/08940886.2016.1198669>.
- [10] H Yan et al., *J Phys Appl Phys* 47 (2014) <https://doi.org/10.1088/0022-3727/47/26/263001>.
- [11] H Yan et al., *Opt Express* 19 (2011) <https://doi.org/10.1364/OE.19.015069>.

- [12] H Yan et al., *Opt Express* 25 (2017) <https://doi.org/10.1364/OE.25.025234>.
- [13] E Nazaretski et al., *Rev Sci Instrum* 84 (2013) <https://doi.org/10.1063/1.4774387>.
- [14] D Shu et al., *J Phys Conf Ser* 463 (2013) <https://doi.org/10.1088/1742-6596/463/1/012029>.
- [15] E Nazaretski et al., *Rev Sci Instrum* 85 (2014) <https://doi.org/10.1063/1.4868968>.
- [16] E Nazaretski et al., *J Synchrotron Radiat* 22 (2015) <https://doi.org/10.1107/S1600577514025715>.
- [17] E Nazaretski et al., *J Synchrotron Radiat* 24 (2017) <https://doi.org/10.1107/S1600577517011183>.
- [18] A Michelson et al., *Science* 376 (2022) <https://doi.org/10.1126/science.abk0463>.
- [19] S Niese et al., *Opt Express* 22 (2014) <https://doi.org/10.1364/OE.22.020008>.
- [20] A Kubec et al., *J Synchrotron Radiat* 21 (2014) <https://doi.org/10.1107/S1600577514014556>.
- [21] E Nazaretski et al., *Appl Phys Lett* 108 (2016) <https://doi.org/10.1063/1.4955022>.
- [22] A Kubec et al., *J Synchrotron Radiat* 24 (2017) <https://doi.org/10.1107/S1600577517001722>.
- [23] W Xu et al., *Opt Express* 28 (2020) <https://doi.org/10.1364/OE.389555>.
- [24] W Xu et al., *Micromachines* 11 (2020) <https://doi.org/10.3390/mi11100939>.